The British Journal of Radiology, 85 (2012), 187–192

PICTORIAL REVIEW

Imaging of desmoplastic small round cell tumour in adults

[1,2]B KIS, MD, PhD, [2]K N O'REGAN, MD, [3]A AGOSTON, MD, PhD, [1,2]O JAVERY, MD, [2]J JAGANNATHAN, MD and [2]N H RAMAIYA, MD

[1]*Department of Radiology, Brigham and Women's Hospital,* [2]*Department of Imaging, Dana Farber Cancer Institute, and* [3]*Department of Pathology, Brigham and Women's Hospital, MA, USA*

ABSTRACT. Desmoplastic small round cell tumour (DSRCT) belongs to the histological descriptive category of small round blue cell tumours. DSRCT primarily occurs in adolescents and young adults between the ages of 15 and 25 years and has a male predominance. DSRCT is an aggressive disease with a poor prognosis; timely diagnosis is therefore critical to the management of these patients. Although their radiographic appearances overlap with other aggressive malignancies, there are certain imaging features that can suggest the diagnosis and expedite the initiation of appropriate therapy. The aim of our pictorial review is to describe the imaging findings of primary and metastatic DSRCT in adults.

Received 8 February 2011
Revised 7 June 2011
Accepted 23 June 2011

DOI: 10.1259/bjr/57186741

Desmoplastic small round cell tumour (DSRCT) belongs to the histological descriptive category of ''small round blue cell tumours'', which include DSRCT, neuroblastoma, Wilms' tumour, rhabdomyosarcoma, Ewing sarcoma, primitive neuroectodermal tumour, small cell osteosarcoma, poorly differentiated synovial cell sarcoma and lymphomas. These malignant tumours are united by their similar histological appearance, which is characterised by sheets of small cells with round nuclei.

DSRCT was first described as a distinct pathological entity in 1991 by Gerald et al [1]. DSRCT classically occurs in adolescents and young adults between the ages of 15 and 25 years and has a male predominance (male:female ratio of 4:1) [2, 3]. Patients usually present with vague abdominal or pelvic discomfort and occasionally a palpable abdominal mass. The primary tumour typically arises in the peritoneal cavity of the pelvis, although DSRCT arising from other sites has been described (including the brain, lung, pleura, stomach, pancreas, ovary, paranasal sinuses and scrotum) [4]. DSRCT is an aggressive disease with a poor prognosis and a mean survival time of 23 months [3]. Timely diagnosis is therefore critical to the management of these patients.

Microscopically, the tumour consists of solid nests of uniform small cells with round hyperchromatic nuclei and clear cytoplasm surrounded by a desmoplastic stroma consisting of fibroblasts and hyperplastic blood vessels (Figure 1a). DSRCT immunohistochemistry shows characteristic polyphenotypic differentiation evidenced by coexpression of epithelial, mesenchymal and neural markers [5] (Figure 1b–d). The tumour is genetically defined by the specific reciprocal translocation between chromosomes 11 and 22, leading to fusion of the Ewing sarcoma gene (EWS) and Wilms' tumour gene (WT1) [t(11;22)(q13;p12)] [6]. Reciprocal translocation of the EWS gene is also seen in Ewing sarcoma and primitive neuroectodermal tumours, but there is a separate locus on chromosome 11. Although the radiographic appearance overlaps with other aggressive malignancies, there are certain imaging features that can suggest the diagnosis and therefore expedite the initiation of appropriate therapy. The aim of our pictorial review is to describe imaging findings of primary and metastatic DSRCT in adults.

Address correspondence to: Dr Bela Kis, Department of Radiology, Brigham and Women's Hospital, 75 Francis Street, Boston, MA 02115, USA. E-mail: bkis@partners.org

Imaging

The most common CT findings of DSRCT are single or multiple intraperitoneal soft-tissue masses without an apparent organ of origin. The primary tumour usually arises in the retrovesical or rectouterine space (Figures 2a,b,3c). Areas of low attenuation and non-enhancement are often present representing necrosis, haemorrhage or fibrous components (Figure 2a,b). Foci of calcification can be seen both in the primary tumour and in metastatic deposits (Figures 2a and 4) [2]. The primary mode of spread is by peritoneal seeding and/or metastases to abdominal and pelvic lymph nodes (Figures 2–6). As the disease advances, extensive tumour implants can be seen throughout the peritoneum, typically in the omentum and mesentery (Figures 2, 4−6) [3]. Sometimes peritoneal sarcomatosis can be seen in the form of nodular peritoneal thickening and small volume ascites (Figures 2e,f, 4, 6) [7]. Liver and bone metastases are also common (Figures 2c–f, 4b,c, 6c, 7). Pleural involvement in the form of pleural masses, nodularity and effusion are often seen (Figures 4, 6a). In Tateishi et al's [2] study of four patients they reported 100% incidence of pleural involvement, while

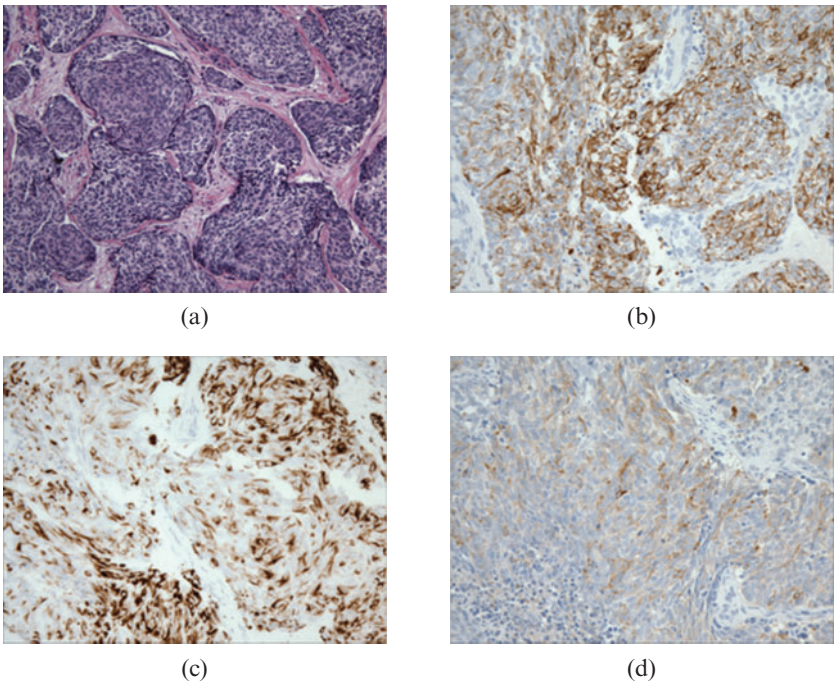

Figure 1. Photomicrograph of haematoxylin-eosin stain (original magnification, ×20) of a pelvic tumour from a 29-year-old male shows (a) nests of uniform small cells with round hyperchromatic nuclei and clear cytoplasm surrounded by a desmoplastic stroma. The tumour shows characteristic polyphenotypic differentiation evidenced by co-expression of epithelial (b, cytokeratin AE1/AE3 stain), mesenchymal (c, desmin staining) and neural markers (d, synaptophysin).

Bellah et al [3] reported 25% incidence in a group of 11 patients. This difference may be due to the different patient populations in each of the respective studies; notably, the age range of patients in Tateishi et al's [2] study was 18–32 years compared with 10–20 years in the study of Bellah et al [3]. In our patient population, of the eight adults (age range, 19–31 years; mean, 26 years), five patients developed pleural involvement (63%). Local mass effect from bulky metastases is not uncommon and, depending on their location, can lead to biliary (Figure 2c,d) or urinary obstruction (Figure 5a). The highly aggressive nature of the tumour is also exemplified by a predilection for seeding of biopsy tracts or surgical incision sites (Figure 5b). Malignant peritoneal mesothelioma, rhabdomyosarcoma and lymphoma can have a similar radiographic appearance to DSRCT and should be considered in the differential diagnosis. Gastrointestinal stromal tumour can have a similar appearance; however, it rarely metastasises to lymph nodes.

MRI can be helpful in delineating the extent of the disease, if surgical resection is considered. DSRCTs often demonstrate high signal intensity on T_2 weighted sequences (Figure 7a). DSRCTs are hypo- or isointense relative to skeletal muscle on T_1 weighted images. Heterogeneous T_1 and T_2 signal patterns and heterogeneous enhancement following gadolinium administration are attributed to fibrous stroma and internal degeneration including necrosis, haemorrhage and calcification [1] (Figure 7a,b). Intratumoural haemorrhage can be seen as a high signal on T_1 weighted images or fluid–fluid levels on T_2 weighted images.

The role for position emission tomography (PET)-CT is not well established in DSRCT imaging. DSRCTs typically show intense fluorodeoxyglucose (FDG) uptake (Figures 6c, 8); thus PET-CT could have a role in the staging and management of these patients. There are four case reports in the literature in which PET-CT was used in the follow-up of DSRCT [8–11]. Each of these case reports found PET-CT to be a very valuable tool for evaluating the progression of metastatic disease and response to chemotherapy. Ben-Sellem et al [8] reported detection of earlier tumoural relapse with PET-CT than with conventional anatomical imaging.

There is no clear consensus regarding the treatment of DSRCT. Given that it is a rare disease, there have been no large-scale randomised trials, and our knowledge is based on a small series of patients in whom the outcomes are highly variable depending on the extent of the disease, resectability and type of therapy. In general, similar to other forms of aggressive sarcomas, treatment involves multimodality therapy including systemic chemotherapy, debulking surgery if possible and sometimes even radiation therapy [12]. Although initial tumour regression was seen in several patients (Figure 3), this favourable response to chemotherapy was transient and the disease was almost always fatal.

Conclusion

DSRCT is a rare childhood sarcoma which can occur in adults. The radiologist should consider this diagnosis when a dominant intraperitoneal soft-tissue mass is seen without an apparent organ of origin with lymphadenopathy, mesenteric nodules and peritoneal spread. Other characteristic features include possible calcification in both primary and metastatic masses, heterogeneous enhancement and development of peritoneal sarcomatosis. Although CT is the mainstay of imaging for DSRCT, PET-CT may be considered in DSRCT follow-up imaging.

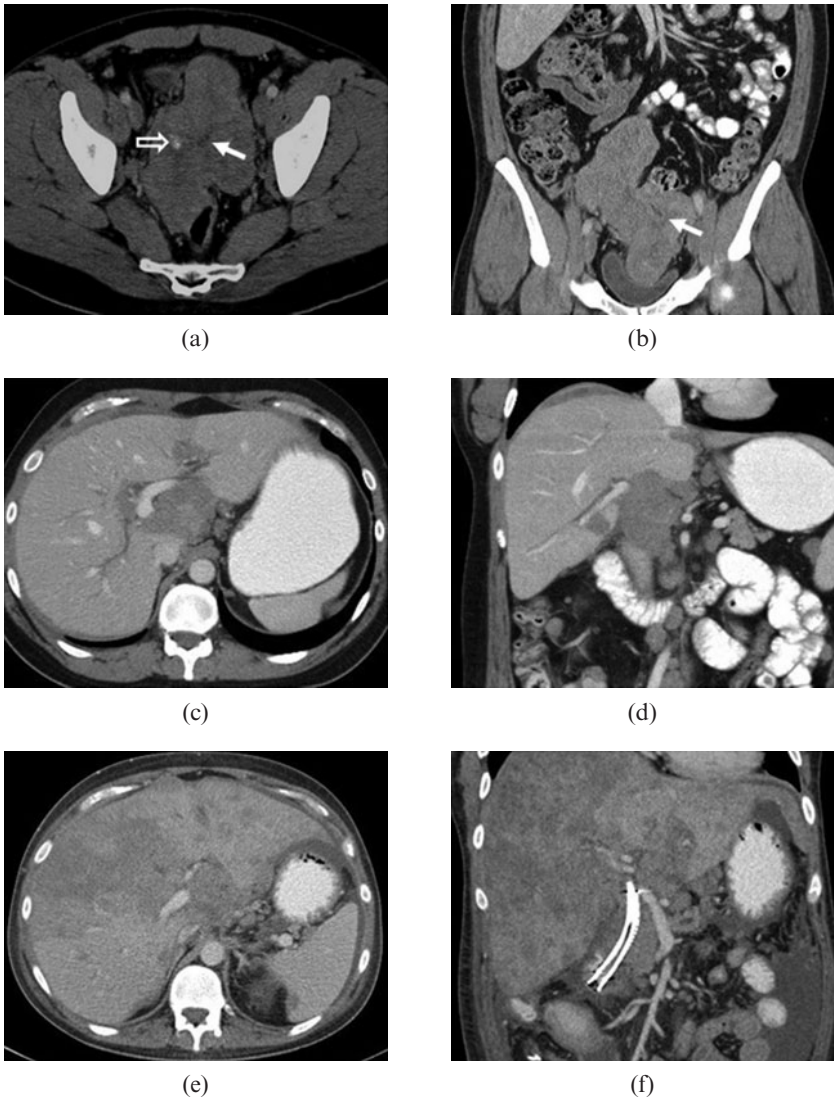

Figure 2. 29-year-old male presented with right upper quadrant discomfort. Initial contrast-enhanced (a) axial and (b) coronal CT images show a large heterogeneous lobulated mass in the pelvis with foci of calcification (open arrow) and multiple soft-tissue masses within the pelvis and mesentery. Central stellate low density area corresponds to an area of fibrosis (solid arrows). As the disease progressed the patient developed biliary obstruction and intrahepatic biliary ductal dilation as a result of metastatic disease in the porta hepatis (c,d) and then extensive hepatic metastatic disease (e,f). The patient died 27 months after initial diagnosis.

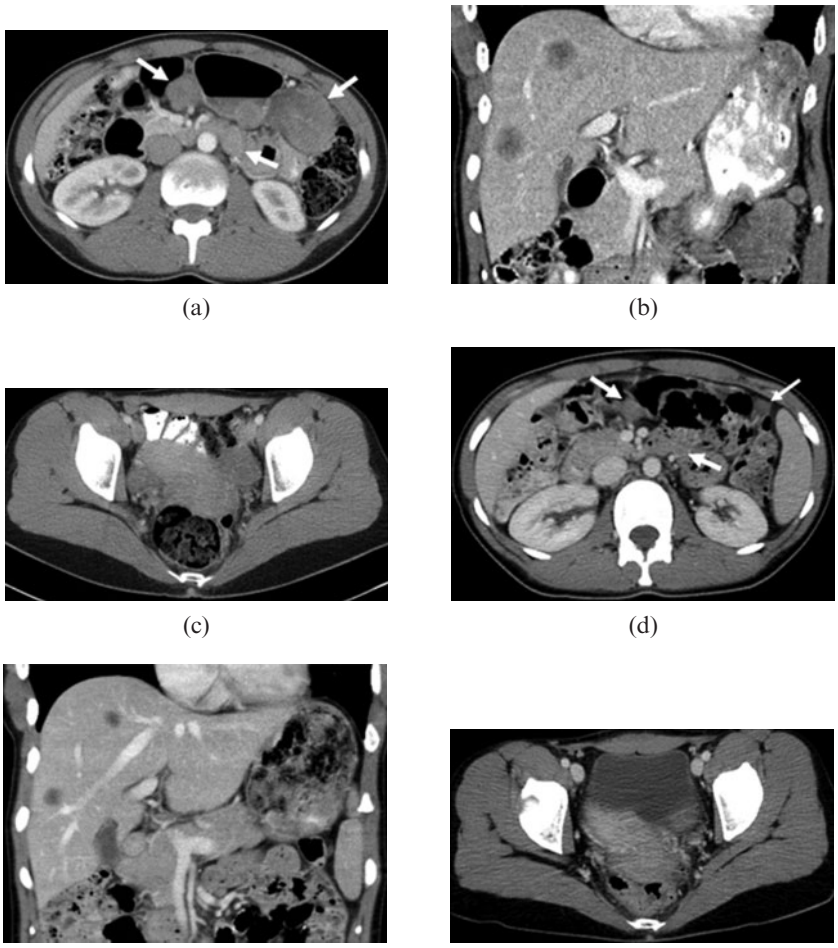

Figure 3. An otherwise healthy 26-year-old female presented with enlarged right external iliac lymph nodes. (a–c) Initial contrast-enhanced CT shows a dominant mass in the rectouterine space inseparable from the uterus and multiple smaller intraperitoneal soft-tissue masses, enlarged retroperitoneal lymph nodes and metastatic disease in the liver. (d–f) After four cycles of chemotherapy the lesions are significantly decreased in size. Arrows indicate representative lesions.

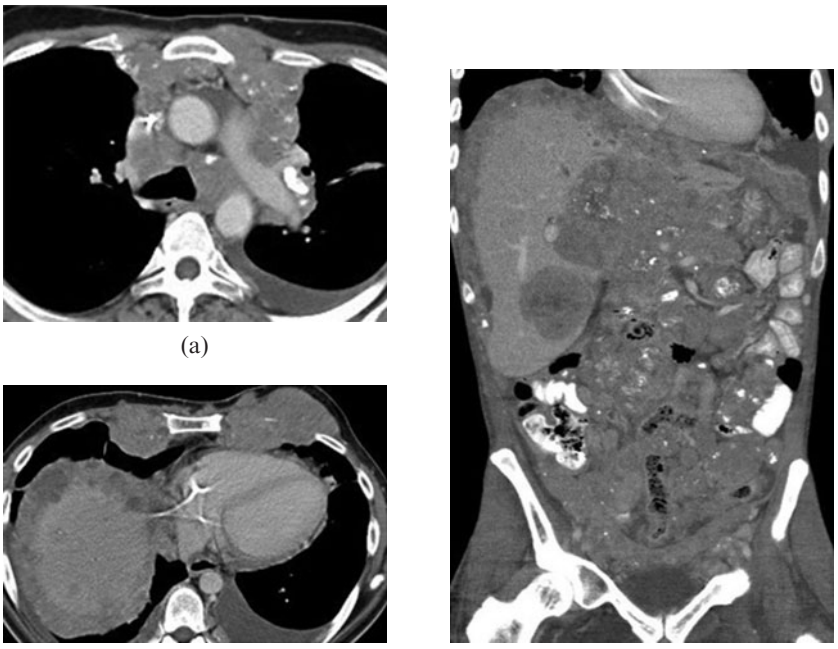

Figure 4. 29-year-old male originally presented with abdominal pain and weight loss. Later in the course of the disease the patient developed left pleural effusion and extensive metastatic disease involving mediastinal (a) lymph nodes, (b) ribs, (b,c) liver and (c) innumerable peritoneal and mesenteric implants. Many of the metastatic masses contain foci of calcifications.

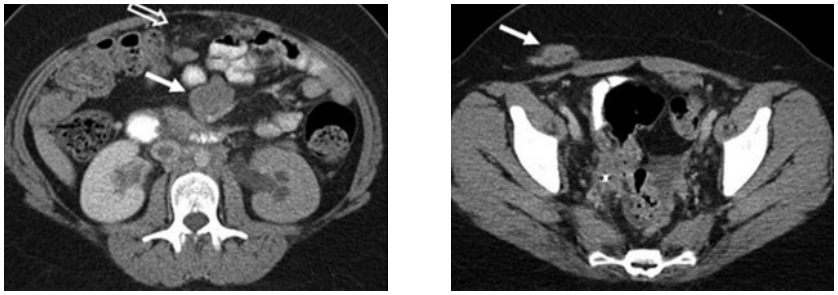

(a) (b)

Figure 5. 23-year-old female who was found incidentally to have multiple retroperitoneal and perihepatic masses in an abdominal CT following a motor vehicle collision. (a) Axial contrast-enhanced CT image shows moderate bilateral hydronephrosis due to distal ureteral obstruction by retroperitoneal masses (not shown). Large mesenteric mass is also seen (a, solid arrow). Nodularity is seen in the omentum (a, open arrow). The patient also developed a metastatic subcutaneous soft-tissue mass along the surgical incision of a prior open biopsy (b, solid arrow).

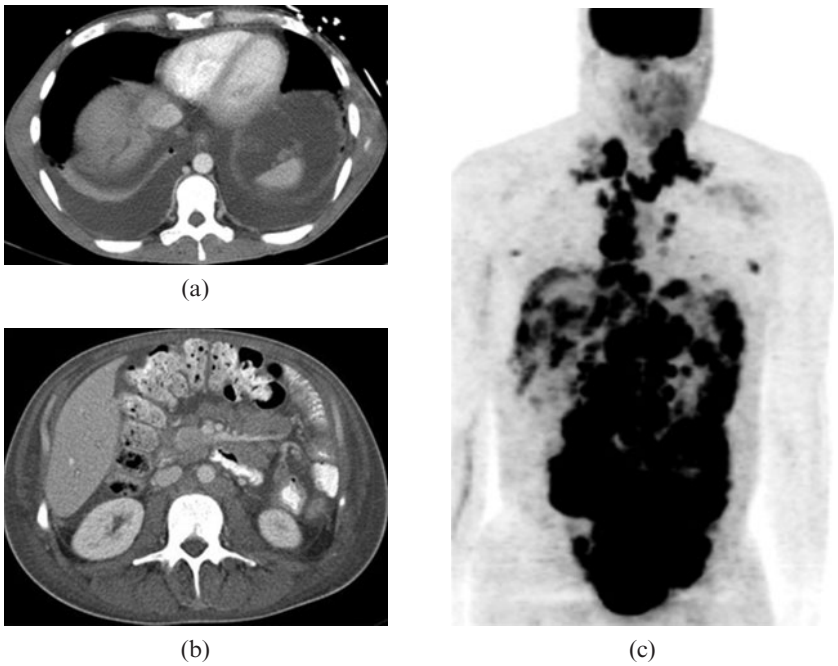

(a) (b) (c)

Figure 6. 28-year-old male presented with left groin lymphadenopathy and weight loss. (a,b) Axial contrast-enhanced CT images show moderate bilateral pleural effusion, pleural thickening and nodularity, ascites, retroperitoneal and mesenteric adenopathy. (c) Coronal maximum intensity projection positron emission tomography image reveals diffuse metastatic disease.

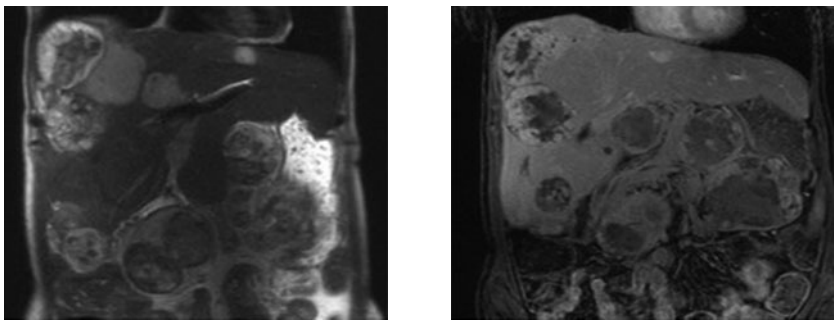

(a) (b)

Figure 7. 25-year-old female with metastatic desmoplastic small round cell fumour. (a) Coronal half Fourier acquisition single-shot turbo spin-echo and (b) gadolinium-enhanced MRI show multiple lesions in the liver, which are heterogeneously hyperintense on (a) T_2 weighted images and (b) demonstrate heterogeneous enhancement with central necrosis.

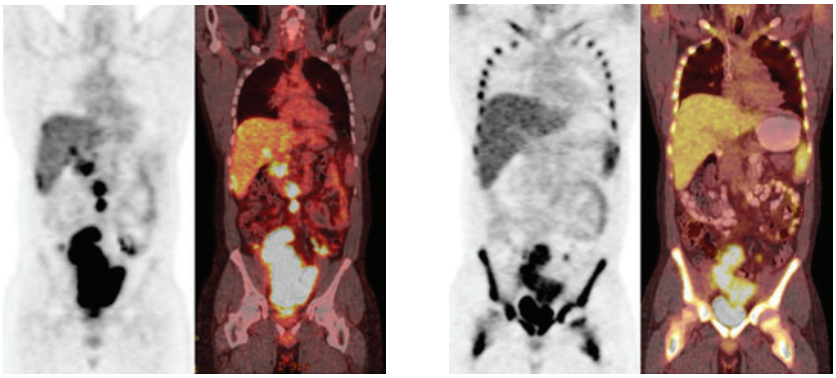

(a) (b)

Figure 8. 29-year-old male presented with right upper quadrant discomfort. (a) Coronal maximum intensity projection positron emission tomography (PET) image and coronal fused PET-CT image of initial PET-CT study shows avid flurodeoxyglucose (FDG) uptake in a large lobulated mass in the pelvis (maximum standardised uptake value (SUV_{max}), 16.5) and multiple FDG-avid retroperitoneal lymph nodes. (b) Follow-up PET-CT following four cycles of chemotherapy FDG uptake in the dominant pelvic mass (SUV_{max}, 8.7) and in the metastatic lymph nodes significantly decreased. The size of the lesions only slightly decreased. The prominent bone marrow uptake in the follow-up PET-CT images is due to granulocyte colony-stimulating factor treatment (b).

References

1. Gerald WL, Miller HK, Battifora H, Miettinen M, Silva EG, Rosai J. Intra-abdominal desmoplastic small round-cell tumour: report of 19 cases of a distinctive type of high-grade polyphenotypic malignancy affecting young individuals. Am J Surg Pathol 1991;15:499–513.
2. Tateishi U, Hasegawa T, Kusumoto M, Oyama T, Ishikawa H, Moriyama N. Desmoplastic small round cell tumour: imaging findings associated with clinicopathologic features. J Comput Assist Tomogr 2002;26:579–83.
3. Bellah R, Suzuki-Bordalo L, Brecher E, Ginsberg JP, Maris J, Pawel BR. Desmoplastic small round cell tumour in the abdomen and pelvis: report of CT findings in 11 affected children and young adults. Am J Roentgenol 2005;184:1910–14.
4. Pickhardt PJ, Fisher AJ, Balfe DM, Dehner LP, Huettner PC. Desmoplastic small round cell tumour of the abdomen: radiologic-histopathologic correlation. Radiology 1999;210: 633–8.
5. Lae ME, Roche PC, Jin L, Lloyd RV, Nascimento AG. Desmoplastic small round cell tumour: a clinicopathologic, immunohistochemical, and molecular study of 32 tumours. Am J Surg Pathol 2002;26:823–35.
6. Gerald WL, Haber DA. The EWS-WT1 gene fusion in desmoplastic small round cell tumour. Semin Cancer Biol 2005;15:197–205.
7. Oei TN, Jagannathan JP, Ramaiya N, Ros PR. Peritoneal sarcomatosis versus peritoneal carcinomatosis: imaging findings at MDCT. Am J Roentgenol 2010;195:W229–35.
8. Ben-Sellem D, Liu K, Cimarelli S, Constantinesco A, Imperial A. Desmoplastic small round cell tumour: impact of 18F-FDG PET induced treatment strategy in a patient with long-term outcome. Rare Tumors 2009;1:31–3.
9. Dimitrakopoulou-Strauss A, Hohenberger P, Ströbel P, Marx A, Strauss LG. A recent application of fluoro-18-deoxyglucose positron emission tomography, treatment monitoring with a mammalian target of rapamycin inhibitor: an example of a patient with a desmoplastic small round cell tumour. Hell J Nucl Med 2007;10:77–9.
10. Rosoff PM, Bayliff S. Successful clinical response to Irinotecan in desmoplastic round blue cell tumour. Med Pediatr Oncol 1999;33:500–3.
11. Kushner BH, Laquaglia MP, Gerald WL, Kramer K, Modak S, Cheung NK. Solitary relapse of desmoplastic small round cell tumour detected by positron emission tomography/computed tomography. J Clin Oncol 2008;26: 4995–6.
12. Hassan I, Shyyan R, Donohue JH, Edmonson JH, Gunderson LL, Moir CR, et al. Intraabdominal desmoplastic small round cell tumours: a diagnostic and therapeutic challenge. Cancer 2005;104:1264–70.